

Research Article

Heat Transfer Optimization of Series-Wound Space Radiators

XueTao Cheng 

Administrative Center of Baohe District, Hefei, 230051, China
E-mail: chengxt02@gmail.com

Received: 2 April 2024; **Revised:** 20 May 2024; **Accepted:** 20 May 2024

Abstract: In spacecraft, the analysis and optimization of space radiators are very important for improving the performance of thermal control system. In this paper, a physical and mathematical model for heat transfer optimization of series-wound space radiators is set up. With the model, a system with five space radiators is optimized to obtain the optimal distributions of total thermal conductance that lead to the maximum heat transfer rate for fixed inlet temperature of the fluid and the minimum inlet temperature of the fluid for fixed heat transfer rate, respectively. The influences of the operation parameters on the optimization results are discussed. When the inlet temperature or the heat transfer rate is fixed, it is shown that the value of total thermal conductance has little effect on the optimal distribution. When the total thermal conductance is fixed, the results show that neither the inlet temperature of the fluid nor the heat transfer rate is an important factor that affects the optimization results. Furthermore, the applicability of the entropy generation minimization and the entransy theory to the analysis of the system is also discussed. Both the theoretical analysis and the numerical results show that the entransy theory is always applicable to the optimization problems, while the entropy generation minimization is not.

Keywords: heat transfer, space radiator, optimization, entransy, entropy generation minimization

1. Introduction

Space radiators are very important in the thermal control system of spacecraft because the waste heat in spacecraft is finally transported into space through the space radiators. Accordingly, the analysis and design of space radiators are of great significance to the improvement of the performance of thermal control system and have attracted much attention from researchers [1-6].

In engineering, when space radiators are analyzed or optimized, there are different design objectives. In some application cases, the focus is the material that gives high thermal emittance [7, 8]. For instance, Kussmaul et al. [7] successfully used the discharge chamber of a 30 cm ion source to texture potential space radiator materials to obtain values of thermal emittance greater than 0.85 at 700 and 900 K. In some cases, the design objective is to improve the heat transfer performance. For instance, Kumar et al. [1] considered a space radiator with uniform area fins standing vertically on a nonisothermal parent surface to enhance heat transfer. Arslanturk [3] used the Adomian decomposition method to evaluate the efficiency of a radiating rectangular fin with variable thermal conductivity and calculated the optimum dimensions of space radiators which maximized the heat transfer rate per unit radiator mass with the corresponding correlation equations. Cheng et al. [9-11] tried to improve the ability of radiative heat transfer

by improving the homogenization of temperature field. Sometimes, the objective is to minimize the system mass. For instance, Xu and Chen [12] set up a physical and mathematical model, including the model of a space radiator, and obtained the design parameters that lead to the minimization of the system mass of heat exchanger networks in spacecraft. For a manned spacecraft, Zhou et al. [13] also set up a mathematical model for the mass of space radiators and minimized the mass of the active thermal control system with the conditional extremum optimization method.

In this paper, we focus on the heat transfer performance and optimize the distribution of total thermal conductance for series-wound space radiators. A physical and mathematical model for the optimization problems is obtained, and the optimal distributions that give the maximum heat transfer rate for fixed inlet temperature of the fluid or the minimum inlet temperature of the fluid for fixed heat transfer rate of the system are calculated, respectively. The entropy generation minimization [14] and the entransy theory [5, 15] are also applied to the analysis. The expressions of the concepts of entropy generation rate, entransy dissipation rate, and entransy-dissipation-based thermal resistance are derived, and the applicability of the concepts to the optimization problems is also discussed.

2. Series-wound space radiators and optimization problems

In engineering, space radiators may be arranged at different locations of spacecraft to release heat into space. In thermal control system of spacecraft, they can be connected by fluid pipes in different ways, such as series, parallel, or hybrid, depending on the practical application conditions. As below, we analyze a group of series-wound space radiators connected by one main pipe, in which the inlet temperature and heat capacity flow rate of the fluid are T_{in} and C , respectively. Assume that there are n space radiators, and the i th space radiator can be shown in Figure 1, in which the red arrow represents the fluid flowing in the pipe, and the direction of the arrow represents the direction of the flow. For the i th space radiator, i is the serial number of the space radiator, the inlet temperature of the fluid is $T_{in,i}$, and the thermal conductance between the fluid and the space radiator is U_i . The heat flow rate Q_i is transported from the fluid into the space radiator, and finally released into the space. Therefore, the total heat transfer rate of the system, Q , can be expressed as

$$Q = \sum_{i=1}^n Q_i \quad (1)$$

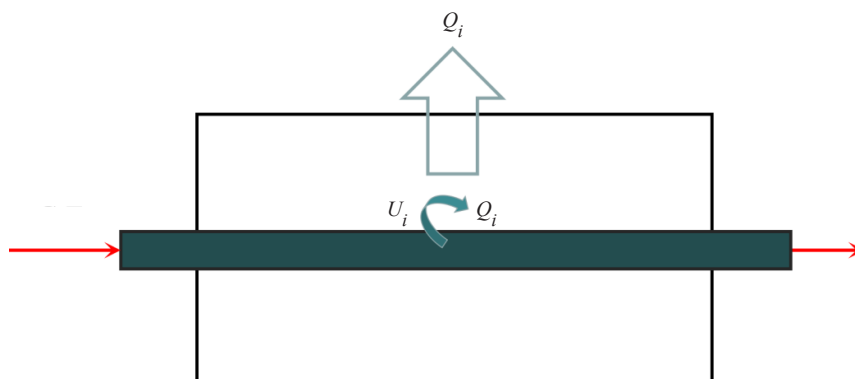


Figure 1. Sketch of the i th space radiator

In the system, the total thermal conductance of the space radiators should be limited with the consideration of the launch cost, so we can assume that

$$U = \sum_{i=1}^n U_i = \text{const} \quad (2)$$

where U is the total thermal conductance. Accordingly, the distribution of total thermal conductance should be optimized to improve the heat transfer performance of the system. When the inlet temperature, T_{in} , is fixed, the best heat transfer performance can mean the maximum total heat transfer rate and the optimization problem can be expressed as

$$\begin{cases} \max Q, \\ \text{s.t. } \sum_{i=1}^n U_i = U \end{cases} \quad (3)$$

When the total heat transfer rate, Q , is fixed, the best heat transfer performance can correspond to the minimum inlet temperature of the fluid, and the corresponding optimization problem can be expressed as

$$\begin{cases} \min T_{\text{in}}, \\ \text{s.t. } \sum_{i=1}^n U_i = U \end{cases} \quad (4)$$

As below, a physical and mathematical model is introduced for the system to analyze the two optimization problems expressed by Eqs. (3) and (4).

3. Physical and mathematical model and optimization method

In Figure 1, it can be seen that the heat transfer system is coupled with the radiative heat transfer process and the heat transfer process between the fluid and the space radiators. To simplify the problem, the heat transfer process between the fluid and the i th space radiator can be treated as that between a hot stream and a cold plate. Therefore, we have [16]

$$Q_i = C(T_{\text{in}-i} - T_i) \left[1 - \exp\left(-\frac{U_i}{C}\right) \right] \quad (5)$$

where T_i is the heat transfer temperature of the space radiator near the fluid. Considering that there are $i - 1$ space radiators before the i th space radiator, we can obtain that

$$C(T_{\text{in}} - T_{\text{in}-i}) = \sum_{j=1}^{i-1} Q_j \quad (6)$$

Therefore,

$$T_{\text{in}-i} = T_{\text{in}} - \frac{\sum_{j=1}^{i-1} Q_j}{C} \quad (7)$$

Accordingly, Eq. (5) can be rewritten as

$$Q_i = C \left(T_{\text{in}} - \frac{\sum_{j=1}^{i-1} Q_j}{C} - T_i \right) \left[1 - \exp\left(-\frac{U_i}{C}\right) \right] \quad (8)$$

On the surface of the space radiator, the temperature would not be uniformly T_i due to the conductive heat transfer process in the space radiator and the radiative heat transfer process between the surface and the space. Therefore, when we calculate the heat transfer rate of radiative heat transfer, the space radiator can be treated as a fin in convective heat transfer. Then, we have

$$Q_i = f_i \left[\sigma \varepsilon_i A_i (T_i^4 - T_S^4) \right] \quad (9)$$

where f_i is the fin efficiency, σ is the Stefan-Boltzmann constant, ε_i is the emissivity, A_i is the heat transfer area, and T_S is the background temperature of the space.

Combing Eqs. (8) and (9) gives

$$f_i \left[\sigma \varepsilon_i A_i (T_i^4 - T_S^4) \right] = C \left(T_{\text{in}} - \frac{\sum_{j=1}^{i-1} Q_j}{C} - T_i \right) \left[1 - \exp\left(-\frac{U_i}{C}\right) \right] \quad (10)$$

Eq. (10) can be rewritten as

$$T_i^4 + \frac{1}{a_i} T_i - \frac{b_i}{a_i} = 0 \quad (11)$$

where

$$a_i = \frac{\sigma f_i \varepsilon_i A_i}{C \left[1 - \exp\left(-\frac{U_i}{C}\right) \right]} \quad (12)$$

$$b_i = \frac{\sigma f_i \varepsilon_i A_i}{C \left[1 - \exp\left(-\frac{U_i}{C}\right) \right]} T_S^4 + T_{\text{in}} - \frac{\sum_{j=1}^{i-1} Q_j}{C} \quad (13)$$

With the equations above, the physical and mathematical model for the coupled heat transfer process is obtained. First, we can analyze the optimization problem in Eq. (3) with the model. In this case, we assume that the heat capacity flow rate, the fin efficiency, the emissivity, the heat transfer area for radiative heat transfer and the background temperature of the space are all given for the i th space radiator. For every distribution of total thermal conductance, a_i is obviously fixed. Meanwhile, for the first space radiator, b_1 is also fixed because the inlet temperature of the fluid is given. Accordingly, solving Eq. (11) gives T_1 . With Eq. (8) or (9), the heat transfer rate of the first space radiator, Q_1 , can be obtained. Then, it can be seen with Eq. (13) that b_2 is also fixed, and T_2 and Q_2 can be further calculated. In this way, the values of b_i , T_i and Q_i can all be obtained.

To find the value of T_i , we should solve Eq. (11), which is a quartic equation about T_i . As below, we solve it numerically. According to Eq. (11), we can have a function,

$$F(T_i) = T_i^4 + \frac{1}{a_i}T_i - \frac{b_i}{a_i} \quad (14)$$

If we draw the curve of the function, $F(T_i)$, we can find that the solution of Eq. (11) is the value of the abscissa of the intersection of the curve and the horizontal axis. In our calculation, an initial value of T_i , T_{i-0} , can be first given, and the point $(T_{i-0}, F(T_{i-0}))$ can be obtained. Considering that there is

$$\frac{dF}{dT_i} = 4T_i^3 + \frac{1}{a_i} \quad (15)$$

we can obtain the slope of the tangent of the curve at the point $(T_{i-0}, F(T_{i-0}))$,

$$k_{i-0} = 4T_{i-0}^3 + \frac{1}{a_i} \quad (16)$$

Therefore, the equation of the tangent can be expressed as

$$y - F(T_{i-0}) = k_{i-0}(x - T_{i-0}) \quad (17)$$

where x is the abscissa, and y is the ordinate. The abscissa of the intersection of the tangent and the x -axis is

$$x_{i-1} = T_{i-0} - \frac{F(T_{i-0})}{k_{i-0}} \quad (18)$$

Then, let $T_{i-1} = x_{i-1}$, and a new point, $(T_{i-1}, F(T_{i-1}))$, can be obtained. Repeating the processes from Eq. (16) to Eq. (18) gives the abscissa of the intersection of the x -axis and the new tangent at point $(T_{i-1}, F(T_{i-1}))$. In this way, T_{i-m} can be obtained after m iterations, and can be treated as the solution of Eq. (11) when there is

$$|F(T_{i-m})| < \delta \quad (19)$$

where δ is a very small quantity and can be set to be 1×10^{-6} in our calculation.

Furthermore, in the constraint equation, Eq. (2), it can be seen that there are n variables that are not independent of each other. Let

$$\left\{ \begin{array}{l}
U_1 = Up_1, p_1 \in [0, 1] \\
U_2 = U(1-p_1)p_2, p_2 \in [0, 1] \\
U_3 = U(1-p_1)(1-p_2)p_3, p_3 \in [0, 1] \\
\dots\dots \\
U_i = Up_i \prod_{j=1}^{i-1} (1-p_j), p_i \in [0, 1] \\
\dots\dots \\
U_{n-1} = Up_{n-1} \prod_{j=1}^{n-2} (1-p_j), p_{n-1} \in [0, 1] \\
U_n = U \prod_{j=1}^{n-1} (1-p_j)
\end{array} \right. \quad (20)$$

In this way, the original n variables are replaced by $n - 1$ independent variables that are all in the range of $[0, 1]$. Accordingly, the optimization problem shown in Eq. (3) can be solved by the following steps:

- (1) Give a value of p_1 , and calculate U_1 with Eq. (20).
- (2) Calculate a_1 and b_1 with Eqs. (12) and (13).
- (3) Solve Eq. (11) and obtain T_1 .
- (4) Calculate Q_1 with Eq. (8) or (9).

(5) Repeat the processes from (1) to (4), and calculate the corresponding parameters from the second space radiator to the last one. For instance, give a value of p_2 for the second space radiator, and calculate U_2 ; Then, calculate a_2 and b_2 with U_2 and Q_1 ; Solve Eq. (11) and obtain T_2 , and then calculate Q_2 . The heat transfer rates of the other space radiators can also be obtained in this way.

- (6) Calculate the total heat transfer rate, Q , with Eq. (1).

(7) For different groups of the values of the $n - 1$ independent parameters, p_i , in the range of $[0, 1]$, different distributions of total thermal conductance and the corresponding total heat transfer rates can all be calculated. Compare all the total heat transfer rates, and obtain the maximum one and the corresponding distribution of total thermal conductance.

Second, the optimization problem shown in Eq. (4) can also be analyzed. The optimization steps are shown below:

- (1) Give an initial value of T_{in} , and turn the problem to an optimization problem expressed by Eq. (3).

(2) Calculate the maximum total heat transfer rate, Q_{max} , and obtain the corresponding optimal distribution of total thermal conductance. Let T_{in} increase by a small value when there is

$$Q_{given} - Q_{max} > c \quad (21)$$

where Q_{given} is the given total heat transfer rate, and c is a small value that can be set to be 1×10^{-2} in our calculation. When there is

$$Q_{given} - Q_{max} < -c \quad (22)$$

let T_{in} decrease by a small value. Then, repeat the calculation of the maximum total heat transfer rate.

- (3) When there is

$$|Q_{\text{given}} - Q_{\text{max}}| < c \quad (23)$$

the corresponding T_{in} and optimal distribution of total thermal conductance can be treated as the optimization results.

With the physical and mathematical model and the optimization method above, some numerical cases can be presented and discussed below.

4. Numerical cases and discussions

First, we present a numerical case with the optimization problem shown in Eq. (3). Assume that $n = 5$, $T_{\text{in}} = 280$ K, $U = 20$ W/K, $C = 2$ W/K, $\varepsilon_i = 0.9$, $A_i = 2$ m², $f_i = 0.8$ and $T_s = 4$ K. In this case, the variations of the total heat transfer rate with different values of p_i are shown in Figure 2. The numerical results show that the maximum total heat transfer rate, 301.39 W, can be obtained when $p_1 = 0.2526$, $p_2 = 0.2916$, $p_3 = 0.3654$ and $p_4 = 0.5212$. Correspondingly, the optimal distribution of total thermal conductance is $U_1 = 5.05$ W/K, $U_2 = 4.36$ W/K, $U_3 = 3.87$ W/K, $U_4 = 3.50$ W/K and $U_5 = 3.22$ W/K. It can be seen that the optimal thermal conductances decrease from the first space radiator to the last one. In the system, the inlet temperature of the fluid decreases with increasing serial number of the space radiator, so we can see that $T_{\text{in-1}} > T_{\text{in-2}} > T_{\text{in-3}} > T_{\text{in-4}} > T_{\text{in-5}}$. Therefore, distributing more thermal conductance to the space radiators with higher inlet temperatures of the fluid is beneficial to the increase of Q .

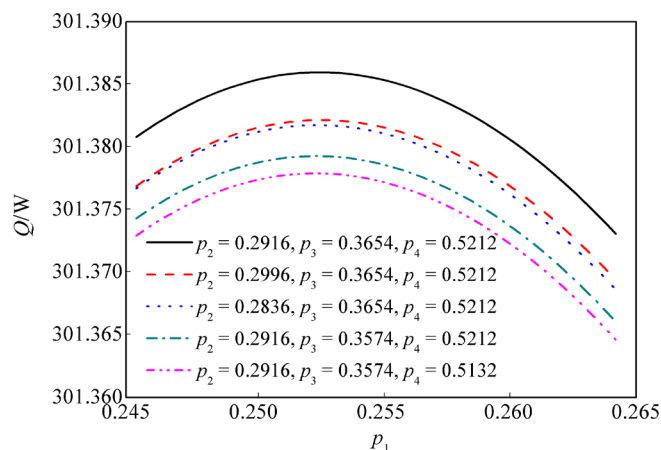


Figure 2. Variations of Q with p_i .

When the total thermal conductance, U , changes, the variations of the maximum Q and the corresponding optimal distributions of U can be calculated and shown in Figure 3. The results show that the optimal U_i increases approximately linearly with increasing U , which means that the increase of U has little effect on the distribution ratio of the optimal U_i for each space radiator. Meanwhile, it can also be seen that the maximum Q increases with increasing U . However, the increase rate of the maximum Q is decreasing. So, there should be a threshold value for U . When U is larger than the threshold value, the influence of U on increasing the maximum Q may become very small. In the present case, 28 W/K can be taken as the threshold value because the increased amount of the maximum Q is less than 1 W when U increases from 28 W/K to 32 W/K.

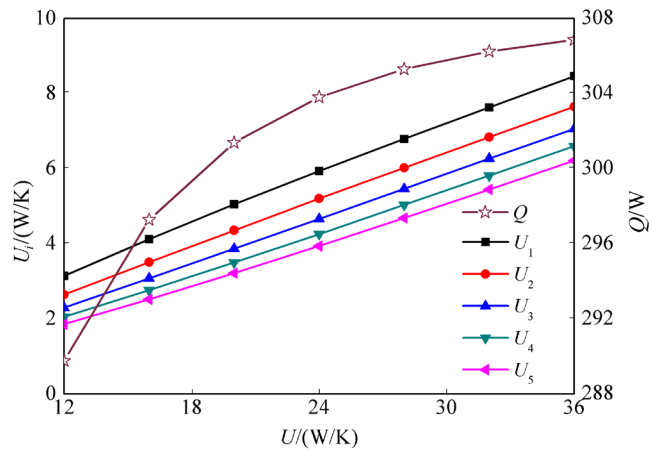


Figure 3. Variations of the maximum Q and the corresponding optimal U_i with U

Furthermore, the influences of the inlet temperature of the fluid, T_{in} , on the maximum heat transfer rate and the corresponding optimal distribution of total thermal conductance are also analyzed. We only change T_{in} , and the other parameters are the same as those of the case shown in Figure 1. Then, the variations of the maximum Q and the corresponding optimal U_i with T_{in} can be obtained and shown in Figure 4. It can be seen that the maximum Q increases approximately linearly when T_{in} increases from 260 K to 310 K, and there is no threshold value. Meanwhile, the optimal U_1 slightly increases from 4.99 W/K to 5.13 W/K, while the optimal U_2 also slightly increases from 4.35 W/K to 4.38 W/K. Correspondingly, the optimal thermal conductances of the third, fourth and fifth space radiators slightly decrease. When T_{in} increases, increasing thermal conductances of the space radiators with smaller serial numbers is beneficial to the increase of Q . As the change amount of the optimal distribution of U is very small, it is clear that T_{in} is not the main factor that affects the optimal distribution of U .

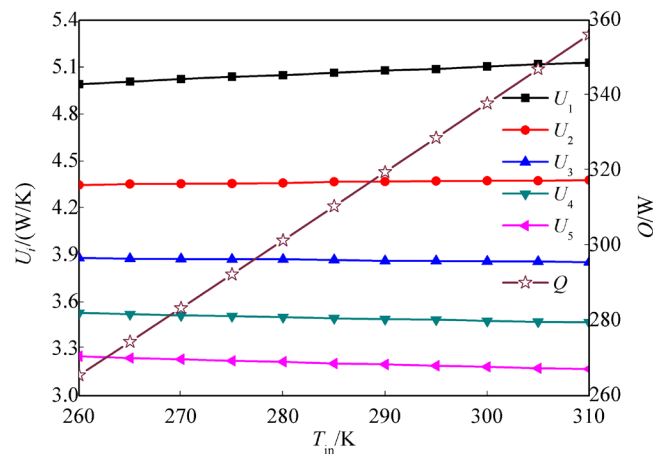


Figure 4. Variations of the maximum Q and the corresponding optimal U_i with T_{in}

Second, we analyze some cases with the problem shown in Eq. (4). It can be seen that Eq. (4) is a reverse problem of the optimization problem shown in Eq. (3). If we assume that $Q = 301.39$ W and the other parameters are the same

as those of the case in Figure 2, we can obtain that the minimum inlet temperature of the fluid, T_{in} , is just 280 K and the optimal distribution of U is the same as that shown in Figure 2. As below, we assume that $n = 5$, $Q = 320$ W, $U = 20$ W/K, $C = 2$ W/K, $\varepsilon_i = 0.9$, $A_i = 2$ m², $f_i = 0.8$ and $T_s = 4$ K. In this case, our numerical results show that the minimum inlet temperature of the fluid, 290.24 K, can be obtained when $p_1 = 0.2540$, $p_2 = 0.2928$, $p_3 = 0.3664$ and $p_4 = 0.5216$. Correspondingly, the optimal distribution of total thermal conductance is $U_1 = 5.08$ W/K, $U_2 = 4.37$ W/K, $U_3 = 3.86$ W/K, $U_4 = 3.49$ W/K and $U_5 = 3.20$ W/K. Here, it can also be seen that the optimal thermal conductances decrease from the first space radiator to the last one for the same reason as that in the case shown in Figure 2.

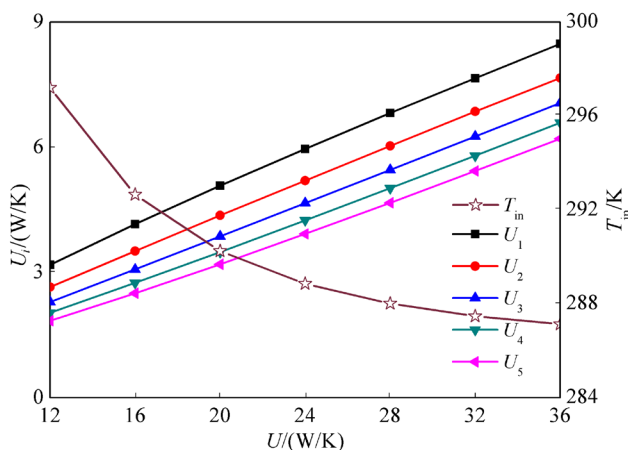


Figure 5. Variations of the minimum T_{in} and the corresponding optimal U_i with U

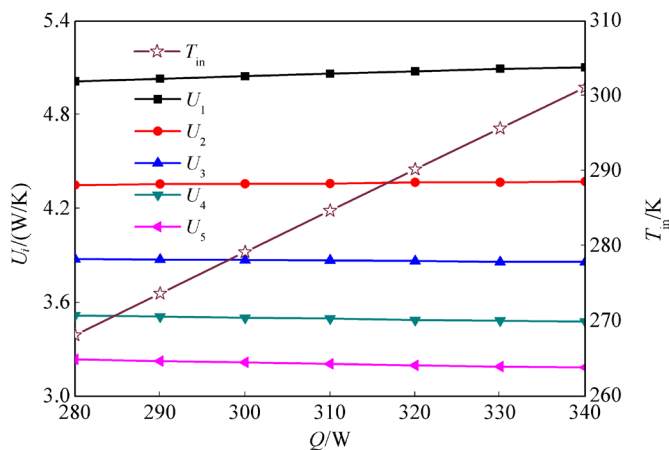


Figure 6. Variations of the minimum T_{in} and the corresponding optimal U_i with Q

When U is a variable, we can also calculate the variations of the minimum T_{in} and the corresponding optimal distributions of U . Assume that $Q = 320$ W, and the results are shown in Figure 5. It can be seen that the optimal U_i increases approximately linearly with increasing U . Therefore, in this case, the increase of U does not have a significant effect on the distribution ratio of the optimal U_i . The results also show that the minimum T_{in} decreases monotonously with increasing U , and there is also a threshold value for U . When U is larger than the threshold value, the influence of

U on decreasing the minimum T_{in} may become very small. In this case, 28 W/K can also be taken as the threshold value because the decreased amount of the minimum T_{in} is less than 1 K when U increases from 28 W/K to 32 W/K.

When Q is a variable, we can assume that $U = 20$ W/K and obtain the variations of the minimum T_{in} and the corresponding optimal U_i . The results are shown in Figure 6. It can be seen that the minimum T_{in} increases approximately linearly with increasing Q , and there is no threshold value, either. As T_{in} increases, the optimal values of U_1 and U_2 increase slightly, while the optimal values of U_3 , U_4 and U_5 decrease by a small amount. Overall, we can see that Q is not an important factor that can affect the optimal distribution of U , either.

5. Entropy generation analysis and entransy analysis

As below, the system is analyzed with the entropy generation minimization and the entransy theory, and the applicabilities of both theories are also discussed.

When the concept of entropy generation is used to analyze the system, there is [17]

$$dS = \delta S_f + \delta S_g \quad (24)$$

where dS is the entropy change with time, δS_f is the entropy flow rate and δS_g is the entropy generation rate. For steady systems, dS equals zero. Therefore,

$$S_g = \int \delta S_g = -\int \delta S_f = S_{f-out} - S_{f-in} \quad (25)$$

where S_{f-in} and S_{f-out} are the entropy flow rates into and out of the system, respectively.

For the system of the series-wound space radiators, the entropy generation rate is composed of three parts,

$$S_g = S_{g-1} + S_{g-2} + S_{g-3} \quad (26)$$

where S_{g-1} is the entropy generation rate due to the convective heat transfer between the fluid and the space radiators, S_{g-2} is that due to the conductive heat transfer in the space radiators, and S_{g-3} is that due to the radiative heat transfer between the surface of the radiators and the space. For the i th space radiator, using Eq. (25) gives the expressions of the corresponding three parts of the entropy generation rate,

$$S_{g-1-i} = \int_{A_{1-i}} \frac{q}{T} dA_{1-i} + C \ln \frac{T_{out-i}}{T_{in-i}} \quad (27)$$

$$S_{g-2-i} = \int_{A_i} \frac{q}{T} dA_i - \int_{A_{1-i}} \frac{q}{T} dA_{1-i} \quad (28)$$

$$S_{g-3-i} = \frac{Q_i}{T_S} - \int_{A_i} \frac{q}{T} dA_i \quad (29)$$

where T_{out-i} and T_{in-i} are the outlet and inlet temperatures of the fluid, A_{1-i} is the area of the boundary through which the heat from the fluid flows into the space radiator, and q is the heat flux. Therefore, we have

$$S_{g-i} = S_{g-1-i} + S_{g-2-i} + S_{g-3-i} = \frac{Q_i}{T_S} + C \ln \frac{T_{out-i}}{T_{in-i}} \quad (30)$$

Then, the total entropy generation rate of the system can be obtained,

$$S_g = \sum_{i=1}^n S_{g-i} = \frac{\sum_{i=1}^n Q_i}{T_S} + C \sum_{i=1}^n \ln \frac{T_{out-i}}{T_{in-i}} = \frac{Q}{T_S} + C \ln \frac{T_{out}}{T_{in}} \quad (31)$$

where T_{out} is the temperature of the fluid at the outlet of the last space radiator.

As there is

$$Q = C(T_{in} - T_{out}) \quad (32)$$

we have

$$S_g = \frac{Q}{T_S} + C \ln \left(1 - \frac{Q}{CT_{in}} \right) \quad (33)$$

When T_{in} is given, there is

$$\frac{dS_g}{dQ} = \frac{1}{T_S} + C \frac{1}{1 - \frac{Q}{CT_{in}}} \times \left(-\frac{1}{CT_{in}} \right) = \frac{1}{T_S} - \frac{1}{T_{in} - \frac{Q}{C}} = \frac{1}{T_S} - \frac{1}{T_{out}} \quad (34)$$

Considering that there must be $T_{out} > T_S$, we can see that Eq. (34) should be positive. Therefore, S_g increases monotonously with increasing T_{in} . Obviously, the entropy generation minimization cannot give the optimal distribution of U for the optimization problem shown in Eq. (3).

On the other hand, when Q is given, we can obtain that

$$\frac{dS_g}{dT_{in}} = C \frac{1}{1 - \frac{Q}{CT_{in}}} \left(-\frac{Q}{C} \right) \left(-\frac{1}{T_{in}^2} \right) = \frac{CQ}{CT_{in}^2 - QT_{in}} = \frac{CQ}{T_{in}(CT_{in} - Q)} = \frac{Q}{T_{in}T_{out}} > 0 \quad (35)$$

In this case, S_g decreases monotonously with decreasing T_{in} . Therefore, the entropy generation minimization can give the optimal distribution of U for the optimization problem shown in Eq. (4).

When the entransy theory [5, 15, 18-35] is used to analyze the system, the entransy balance of the system gives [15, 18]

$$G_{dis} = G_{f-in} - G_{f-out} \quad (36)$$

where G_{dis} is the entransy dissipation rate of the system, G_{f-in} and G_{f-out} are the entransy flow rates into and out of the system, respectively. For the system of the series-wound space radiators, there are also three parts of entransy dissipation,

$$G_{\text{dis}} = G_{\text{dis-1}} + G_{\text{dis-2}} + G_{\text{dis-3}} \quad (37)$$

where $G_{\text{dis-1}}$ is the entransy dissipation rate of the convective heat transfer between the fluid and the space radiators, $G_{\text{dis-2}}$ is that due to the conductive heat transfer in the space radiators, and $G_{\text{dis-3}}$ is that of the radiative heat transfer between the surface of the radiators and the space. With the definition of entransy flow rate for coupled heat transfer processes [5], using Eq. (36) leads to the expressions of the corresponding three parts of the entransy dissipation rate for the i th space radiator,

$$G_{\text{dis-1-}i} = \frac{1}{2}CT_{\text{in-}i}^2 - \int_{A_{1-i}} qTdA_{1-i} - \frac{1}{2}CT_{\text{out-}i}^2 \quad (38)$$

$$G_{\text{dis-2-}i} = \int_{A_{1-i}} qTdA_{1-i} - \int_{A_i} qTdA_i \quad (39)$$

$$G_{\text{dis-3-}i} = \int_{A_i} qTdA_i - Q_iT_S \quad (40)$$

Accordingly, there is

$$G_{\text{dis-}i} = G_{\text{dis-1-}i} + G_{\text{dis-2-}i} + G_{\text{dis-3-}i} = \frac{1}{2}C(T_{\text{in-}i}^2 - T_{\text{out-}i}^2) - Q_iT_S \quad (41)$$

Then, with the consideration that $T_{\text{out-}i}$ equals the inlet temperature of the next space radiator, the entransy dissipation rate of the system can be obtained,

$$G_{\text{dis}} = \sum_{i=1}^n G_{\text{dis-}i} = \frac{1}{2}C \sum_{i=1}^n (T_{\text{in-}i}^2 - T_{\text{out-}i}^2) - T_S \sum_{i=1}^n Q_i = \frac{1}{2}C(T_{\text{in}}^2 - T_{\text{out}}^2) - QT_S \quad (42)$$

Eq. (42) can be rewritten as

$$\begin{aligned} G_{\text{dis}} &= \frac{1}{2}C(T_{\text{in}} - T_{\text{out}})(T_{\text{in}} + T_{\text{out}}) - QT_S \\ &= Q\left(T_{\text{in}} - \frac{Q}{2C}\right) - QT_S \\ &= Q\left(T_{\text{in}} - \frac{Q}{2C} - T_S\right) \end{aligned} \quad (43)$$

The entransy-dissipation-based thermal resistance [15] can also be obtained,

$$R = \frac{G_{\text{dis}}}{Q^2} = \frac{T_{\text{in}} - T_S}{Q} - \frac{1}{2C} \quad (44)$$

When T_{in} is given, there is

$$\frac{dG_{\text{dis}}}{dQ} = T_{\text{in}} - \frac{Q}{C} - T_{\text{S}} = T_{\text{out}} - T_{\text{S}} > 0 \quad (45)$$

Obviously, G_{dis} increases monotonously with increasing Q . Meanwhile, Eq. (45) shows clearly that R always decreases with increasing Q . On the other hand, when Q is given, it is very easy to see with Eqs. (44) and (45) that both G_{dis} and R always decrease monotonously with decreasing T_{in} . Therefore, both the extremum entransy dissipation principle and the minimum entransy-dissipation-based thermal resistance principle are applicable for optimizing the problems shown in Eqs. (3) and (4).

In the cases calculated in Section 4, $C = 2 \text{ W/K}$ and $T_{\text{S}} = 4 \text{ K}$. Therefore, when T_{in} is given and assumed to be 280 K, the variations of S_{g} , G_{dis} and R with Q can be calculated and shown in Figure 7. It can be seen that both S_{g} and G_{dis} increase with increasing Q , while R decreases monotonously. When T_{in} is a variable, the variations of the maximum Q and the corresponding S_{g} , G_{dis} and R can also be obtained and shown in Figure 8. With the increase of T_{in} , the results show that the maximum Q and the corresponding S_{g} and G_{dis} all increase, while R decreases.

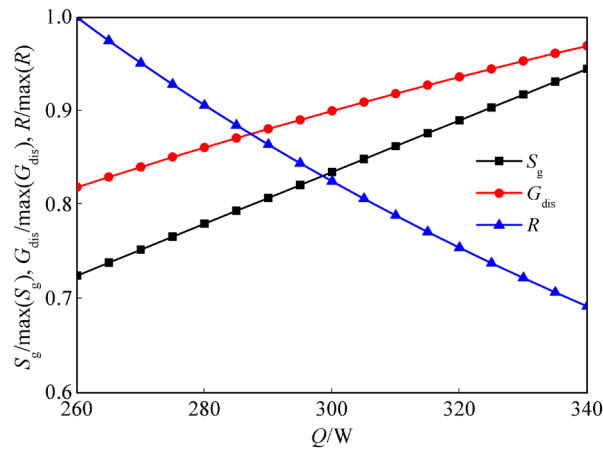


Figure 7. Variations of S_{g} , G_{dis} and R with Q for fixed T_{in}

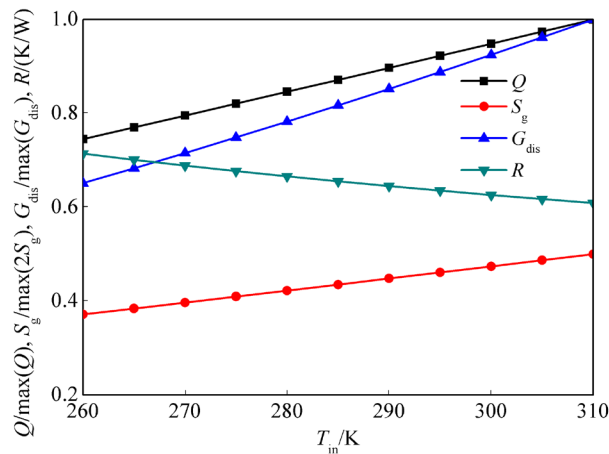


Figure 8. Variations of the maximum Q and the corresponding S_{g} , G_{dis} and R with T_{in}

On the other hand, when Q is fixed and assumed to be 320 W, the variations of S_g , G_{dis} and R with T_{in} can be calculated and shown in Figure 9. It can be found that all three parameters decrease with decreasing T_{in} . When Q is a variable, the variations of the minimum T_{in} and the corresponding S_g , G_{dis} and R can also be calculated and shown in Figure 10. With the increase of Q , the minimum T_{in} and the corresponding S_g and G_{dis} all increase, while R decreases.

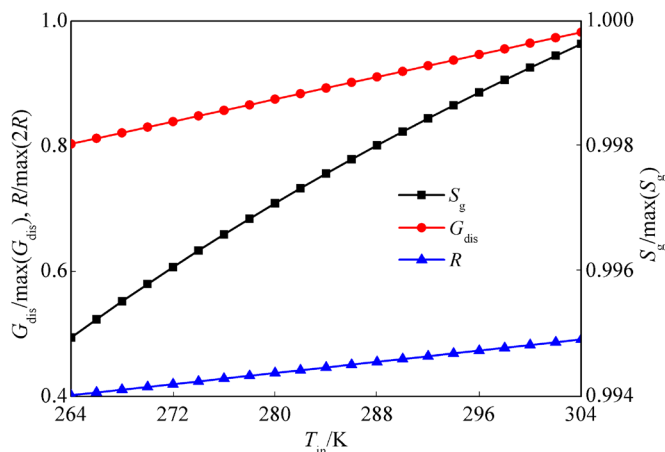


Figure 9. Variations of S_g , G_{dis} and R with T_{in} for fixed Q

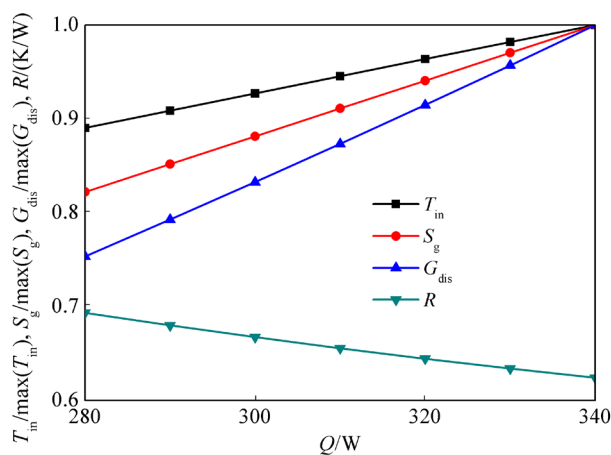


Figure 10. Variations of the minimum T_{in} and the corresponding S_g , G_{dis} and R with Q

Obviously, the theoretical analysis can be verified by the numerical cases above. It can be concluded that the entropy generation minimization is not always applicable to the optimization problems discussed in this paper, but the entransy theory is. Similar conclusions have also been obtained when the entransy theory [5, 15, 21-23] was used to analyze or optimize some other systems [24-28], including heat-work conversion systems [24, 25] and heat transfer systems [28].

6. Conclusions

In this paper, series-wound space radiators are analyzed and optimized to improve the heat transfer performance. A physical and mathematical model for the heat transfer optimization is obtained. With the model, the distribution of total thermal conductance of the system is optimized to maximize the heat transfer rate for fixed inlet temperature of the fluid or minimize the inlet temperature of the fluid for fixed heat transfer rate. Some numerical cases with five space radiators are presented, and the corresponding optimal distributions of total thermal conductance are successfully obtained.

When the inlet temperature or the heat transfer rate is fixed, the influence of total thermal conductance on the optimal distribution is discussed. It is found that the value of total thermal conductance has little effect on the optimal distribution. Furthermore, there are threshold values for the total thermal conductance. When the total thermal conductance is larger than the threshold value, the influence of total thermal conductance on increasing the maximum heat transfer rate or decreasing the minimum inlet temperature may become very small. When the total thermal conductance is fixed, it is found that neither the inlet temperature of the fluid nor the heat transfer rate is the main factor that affects the optimal distribution of total thermal conductance.

The entropy generation minimization and the entransy theory are also used to analyze the system. The expressions of the entropy generation rate, the entransy dissipation rate, and the entransy-dissipation-based thermal resistance are derived. Both the theoretical analysis and the numerical results show clearly that the extremum entransy dissipation rate and the minimum entransy-dissipation-based thermal resistance always lead to optimal results, while the entropy generation minimization does not always.

Conflict of interest

The author declares no competing financial interest.

References

- [1] Kumar SS, Nayak V, Venkateshan SP. Optimum finned space radiators. *International Journal of Heat and Fluid Flow*. 1993; 14: 191-200.
- [2] Roy SK, Avanic BL. Optimization of a space radiator with energy storage. *International Communications in Heat and Mass Transfer*. 2006; 33(5): 544-551.
- [3] Arslanturk C. Optimum design of space radiators with temperature-dependent thermal conductivity. *Applied Thermal Engineering*. 2006; 26: 1149-1157.
- [4] Ning X, Wang Y, Zhang J, Liu D. An equivalent ground thermal test method for single-phase fluid loop space radiator. *Chinese Journal of Aeronaut*. 2015; 28: 86-92.
- [5] Cheng XT, Liang XG. Analyses of coupled steady heat transfer processes with entropy generation minimization and entransy theory. *International Journal of Heat and Mass Transfer*. 2018; 127: 1092-1098.
- [6] Hemadri VA, Gupta A, Khandekar S. Thermal radiators with embedded pulsating heat pipes: Infra-red thermography and simulations. *Applied Thermal Engineering*. 2011; 31: 1332-1346.
- [7] Kussmaul M, Mirtich MJ, Curren A. Ion beam treatment of potential space materials at the NASA Lewis Research Center. *Surface & Coating Technology*. 1992; 51: 299-306.
- [8] Mirtich MJ, Kussmaul M. Enhanced thermal emittance of space radiators by ion-discharge chamber texturing. *Surface & Coating Technology*. 1987; 33: 511-521.
- [9] Cheng XT, Xu XH, Liang XG. Homogenization design of temperature field for the side surface of a cylindrical satellite. *Journal of Ordnance Equipment Engineering*. 2016; 5: 1-6.
- [10] Cheng XT, Xu XH, Liang XG. Homogenization of temperature field for thermal radiator in space. *Journal of Engineering Thermophysics*. 2010; 31: 1031-1033.
- [11] Cheng XT, Liang XG. Relationship between entransy dissipation of thermal radiation and homogenization of temperature field for thermal radiator in space. *Journal of Engineering Thermophysics*. 2012; 33: 311-314.
- [12] Xu YC, Chen Q. Minimization of mass for heat exchanger networks in spacecrafts based on the entransy dissipation theory. *International Journal of Heat and Mass Transfer*. 2012; 55: 5148-5156.
- [13] Zhou B, Cheng XT, Liang XG. Conditional extremum optimization analyses and calculation of the active thermal

- control system mass of manned spacecraft. *Applied Thermal Engineering*. 2013; 59: 639-647.
- [14] Bejan A. *Entropy Generation Minimization*. Florida: CRC Press; 1995.
- [15] Guo ZY, Zhu HY, Liang XG. Entransy-A physical quantity describing heat transfer ability. *International Journal of Heat and Mass Transfer*. 2007; 50: 2545-2556.
- [16] Chen Q, Wu J, Wang MR, Pan N, Guo ZY. A comparison of optimization theories for energy conservation in heat exchanger groups. *Chinese Science Bulletin*. 2010; 56: 449-454.
- [17] Zhao KH, Luo WY. *Thermotics*. Beijing: Higher Education Press; 2002.
- [18] Cheng XT, Liang XG. Entransy, entransy dissipation and entransy loss for analyses of heat transfer and heat-work conversion processes. *Journal of Thermal Science and Technology*. 2013; 8: 337-352.
- [19] Vakalis S, Patuzzi F, Baratieri M. Introduction of an energy efficiency tool for small scale biomass gasifiers-A thermodynamic approach. *Energy Conversion and Management*. 2017; 131: 1-9.
- [20] Huang ZW, Li ZN, Hwang T, Radermacher R. Application of entransy dissipation based thermal resistance to design optimization of a novel finless evaporator. *Science China: Technological Sciences*. 2016; 59: 1486-1493.
- [21] Wu J, Yang XP. An area method for visualizing heat-transfer imperfection of a heat exchanger network in terms of temperature-heat-flow-rate diagrams. *Science China: Technological Sciences*. 2016; 59: 1517-1523.
- [22] Feng HJ, Chen LG, Xie ZH, Ding ZM, Sun FR. Generalized constructal optimization for secondary cooling process of slab continuous casting based on entransy theory. *Science China: Technological Sciences*. 2014; 57: 784-795.
- [23] Wei SH, Chen LG, Xie ZH. Constructal heat conduction optimization: Progresses with entransy dissipation rate minimization. *Thermal Science and Engineering Progress*. 2018; 7: 155-163.
- [24] Kim KH, Kim K. Comparative analyses of energy-exergy-entransy for the optimization of heat-work conversion in power generation systems. *International Journal of Heat and Mass Transfer*. 2015; 84: 80-90.
- [25] Ahmadi MH, Ahmadi MA, Pourfayaz F, Bidi M. Entransy analysis and optimization of performance of nano-scale irreversible Otto cycle operating with Maxwell-Boltzmann ideal gas. *Chemical Physics Letters*. 2016; 658: 293-302.
- [26] Goudarzi N, Talebi S. Heat removal ability for different orientations of single-phase natural circulation loops using the entransy method. *Annual of Nuclear Energy*. 2018; 111: 509-522.
- [27] Xu SZ, Wang RZ, Wang LW. Temperature-heat diagram analysis method for heat recovery physical adsorption refrigeration cycle-Taking multi-stage cycle as an example. *International Journal of Refrigeration*. 2017; 74: 254-268.
- [28] Chen X, Zhao T, Zhang MQ, Chen Q. Entropy and entransy in convective heat transfer optimization: A review and perspective. *International Journal of Heat and Mass Transfer*. 2019; 137: 1191-1220.